



Antibody association with HER-2/*neu*-targeted vaccine enhances CD8⁺ T cell responses in mice through Fc-mediated activation of DCs

Peter S. Kim,^{1,2} Todd D. Armstrong,^{1,3} Hong Song,^{1,4} Matthew E. Wolpoe,^{1,3} Vivian Weiss,^{1,5} Elizabeth A. Manning,^{1,2} Lan Qing Huang,^{1,3} Satoshi Murata,^{1,3} George Sgouros,^{1,4} Leisha A. Emens,^{1,3} R. Todd Reilly,^{1,3} and Elizabeth M. Jaffee^{1,2,3,5}

¹The Sidney Kimmel Comprehensive Cancer Center, ²Department of Pharmacology and Molecular Sciences, ³Department of Oncology, ⁴Department of Radiology and Nuclear Medicine, and ⁵Department of Immunology, Johns Hopkins University School of Medicine, Baltimore, Maryland, USA.

The pathogenic nature of cancer is attributed, at least in part, to the ability of tumor cells to induce systemic and local mechanisms of immune tolerance. However, we previously reported that tumor-free survival in up to 100% of tolerized HER-2/*neu* transgenic mice can be achieved by administration of *neu*-specific mAb concurrently with a HER-2/*neu*-expressing, GM-CSF-secreting whole cell vaccine. In this report, we show that one mechanism of improved antitumor activity induced by the combination of these 2 *neu*-targeted interventions was enhanced Fc-mediated activation of APCs. Specifically, *in vivo* studies demonstrated localization of radiolabeled *neu*-specific mAb at the vaccine site. Subsequently, increased accumulation of *neu*-specific mAb at the vaccine-draining lymph node correlated with increased vaccine cell uptake by DCs *in vivo*. This led to enhancement of CD8⁺ *neu*-specific T cell function in terms of proliferation, cytokine production, and central memory development. Thus, the administration of a *neu*-specific mAb with a *neu*-targeted GM-CSF-secreting tumor vaccine enhanced induction of *neu*-specific CD8⁺ T cells through Fc-mediated activation of DCs. This multimodality attack on the same tumor antigen may have the potential to overcome tolerance to self antigens and weaken the immunosuppressive networks within the tumor microenvironment.

Introduction

A major challenge in developing effective immunotherapies for cancer treatment is the requirement for bypassing immunosuppressive mechanisms within the tumor microenvironment and reducing immune tolerance to endogenous tumor antigens. The immune system forms a safeguard against the recognition of self antigens by central deletion of highly self-reactive T cells during the early immunological development. Lower affinity T cells or T cells of all affinities for antigens not presented in the thymus escape central deletion but become tolerized in the periphery (1, 2). Higher affinity T cells that also escape central deletion become anergic in the periphery through interactions with Tregs (3, 4). Tumor cells escape immune recognition partly because tumor-associated antigens are endogenously recognized as self molecules. Adding to this immune tolerance hurdle, tumor cells themselves build and maintain an immunosuppressive microenvironment through multiple signaling pathways (4–8). This microenvironment also stems from failure to clear the turnover of apoptotic tumor cells by macrophages. The sol-

uble form of phosphatidylserine, released from apoptotic tumor cells, binds to the phosphatidylserine receptor on macrophages and induces production of various tumor-derived soluble factors, which consequently inhibit activation of APCs and T cells (8). Furthermore, the impaired clearance of apoptotic tumor cells causes production of anti-DNA antibodies to self antigen. This in turn leads to an increase in immature DCs (iDCs) and immature macrophages (iMCs), which promote the generation of CD4⁺CD25⁺ Tregs (8).

Tumor-derived VEGF is one of the chemoattractants of iMCs and iDCs from the bone marrow to the tumor site (9). Once exposed to the tumor microenvironment, these iDCs and iMCs become tumor-associated iDCs and tumor-associated macrophages that ultimately suppress antigen-specific T cell activation and function (10, 11). Tumor-associated iDCs and tumor-associated macrophages travel to the tumor-draining lymph nodes and the spleen, creating an immunosuppressive network throughout the physiological system. In contrast, mature DCs are the most potent APCs capable of activating tumor-specific CD8⁺ T cells, and their ability to enhance antitumor immunity depends on the extent to which iDCs are recruited to the tumor site and matured to cross-prime CD8⁺ T cells. A number of DC-targeted and maturing vaccines have been shown to enhance CD8⁺ T cell activation in preclinical models and are in various phases of clinical testing (12). As one example, whole tumor cells genetically modified to express GM-CSF effectively activate bone marrow-derived iDCs that have the ability to induce a potent systemic immune response that can cure mice of micrometastases (13).

Nonstandard abbreviations used: ADCC, antibody-dependent cellular cytotoxicity; DEAD, direct ex vivo antigen detection; iDC, immature DC; m-, mouse; *neu*, HER-2/*neu*; *neu*-N, HER-2/*neu* transgenic; T_{CM}, central memory T cell; T_{EM}, effector memory T cell; VDLN, vaccine-draining lymph node.

Conflict of interest: This article describes the use of a GM-CSF-secreting tumor vaccine. Although none of the authors have financial interests in this work, Johns Hopkins University receives milestone payments and has the potential to receive royalties in the future.

Citation for this article: *J. Clin. Invest.* 118:1700–1711 (2008). doi:10.1172/JCI34333.

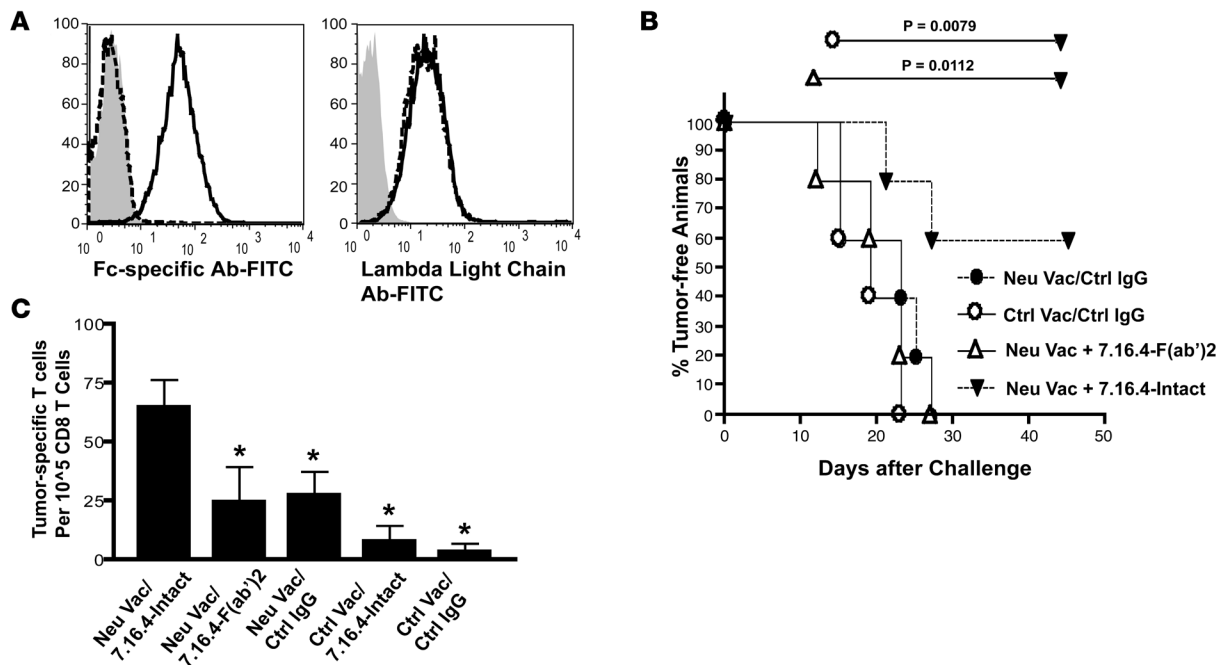


Figure 1

The Fc portion of the intact 7.16.4 mAb is required for enhancement of the vaccine-induced antitumor response. (A) Binding of F(ab')₂ fragments of 7.16.4 (dashed line) were confirmed by flow cytometry, using secondary antibodies specific for the Fc portion and λ₁, λ₂, and λ₃ light chains. Shown are the intact antibody (solid line) and control IgG (gray histogram). (B) Antibody-mediated enhancement of the vaccine-induced antitumor response is not seen in the vaccine + F(ab')₂ treatment group. *neu-N* mice received neu-targeted vaccine (3T3 neu/GM) or control vaccine (3T3 NP/GM), followed 2 weeks later by NT2 challenge + intact 7.16.4 mAb, + 7.16.4 F(ab')₂, + or irrelevant IgG. The intact and control antibodies were administered weekly for a total of 5 injections (100 μg of IgG per injection). F(ab')₂ fragments were injected twice per week for a total of 10 injections [150 μg of F(ab')₂ per injection]. Survival curves are shown (*n* = 5 per group). Statistical differences in survival among data groups were assessed using the log-rank test. This experiment was repeated once. (C) Tumor-specific CD8⁺ T cell responses were not increased in the vaccine + F(ab')₂ treatment group when compared with the vaccine plus intact antibody treatment group. CD8⁺ T cells were incubated with NT2/B7-1 target cells overnight at 37°C at 5% CO₂. IFN-γ ELISPOTS were counted on the next day. Each experiment was repeated 3 times independently. **P* < 0.05 versus intact 7.16.4 mAb + neu-targeted vaccine, Mann-Whitney *U* test.

During the past decade, tumor antigen-specific mAbs have been FDA approved for the treatment of a number of cancers (14). Trastuzumab, an approved neu-targeted mAb that targets HER-2/neu-expressing (neu-expressing) breast cancers and exerts pleiotropic antitumor effects such as inhibiting neu signaling, suppressing angiogenesis, and inducing tumor apoptosis, with the latter mechanism predominate in patients (15). There is increasing evidence that these passively administered mAbs also have immune-modulating effects that augment both humoral and cellular immunity. For example, antibody-dependent cellular cytotoxicity (ADCC) mediated by NK cells has been shown in one in vivo mouse model to be a mechanism by which trastuzumab enhances antitumor immunity (16). Similarly, the efficacy of rituximab, a CD20-targeted mAb, approved for the treatment of lymphoma, is significantly greater in patients with “high responder” Fc receptor polymorphisms, suggesting that the mAb and the Fc receptor are interacting to mediate ADCC (17, 18). In a few preclinical studies, mAbs targeted against a specific tumor antigen have been shown to activate CD8⁺ T cells. This activation is thought to occur via enhanced cross-priming by APCs. DCs in particular efficiently process externally acquired antigens and present them via enhanced cross-priming on MHC class I molecules on their cell surface to enhance T cell activation.

Similar to other APCs, DCs serve as a link to the adaptive immune system. DCs express the low-affinity FcγRIII, the high-affinity FcγRI, and the complement receptor 3 and mannose receptor. These receptors are at their disposal to phagocytose a wide range of foreign molecules and pathogens (19). Both FcγR- and CR-mediated phagocytosis require formation of immune complexes. Phagocytosis is a highly selective process that requires specific interaction between the surface of the particle to be ingested and the plasma membrane of the phagocytic cell (20). Immune complexes bind directly to FcγRs to initiate phagocytic signal transduction, ultimately leading to actin polymerization and pseudopod formation. Extensive studies have been performed to characterize the interaction between the immune complex and FcγR. Various in vitro and in vivo studies have shown that the activation of FcγRs through the binding of immune complexes can lead to an enhanced antigen presentation in DCs (21–26).

Using HER-2/*neu* transgenic (*neu-N*) mice as a clinically relevant model of immune tolerance, we previously reported the observation that combining neu-specific antibodies with neu-targeted, GM-CSF-secreting vaccination effectively increases neu-directed CD8⁺ effector function and tumor-free survival (27). Here, we provide an in-depth analysis of the contribution of DCs to the immune complex-mediated enhanced induction of these tumor-specific CD8⁺ T cell responses. Specifically, we show that the neu antigen/mAb

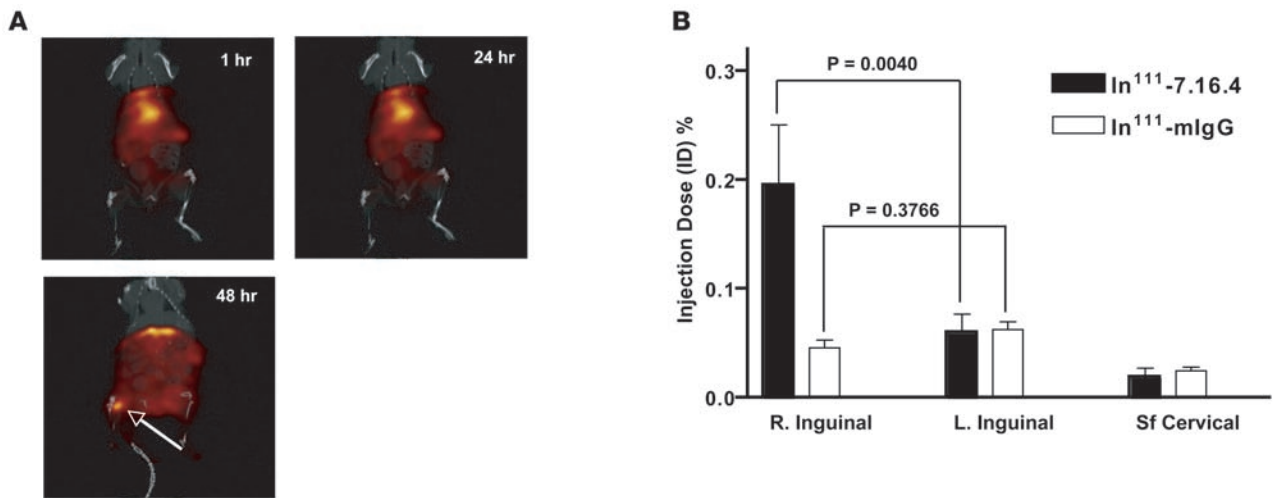


Figure 2 Intact 7.16.4 mAb accumulates preferentially within the draining lymph nodes of neu-expressing, GM-CSF–secreting tumor vaccine cells. **(A)** Indium-111–labeled intact 7.16.4 mAb forms a hot spot (arrow) at the location of the vaccine. *neu-N* mice were given the neu vaccine cells (3T3 neu/GM) (1×10^6) in the right leg or the control GM-CSF–secreting vaccine cells (3T3 NP/GM) (1×10^6) in the left leg s.c., concurrent with an i.v. injection of indium-111–labeled intact 7.16.4 mAb. The SPECT/CT images, using an XPECT system, were taken at 1, 24, and 48 hours. Three mice per group were analyzed per experiment, and these experiments were repeated once with similar results. **(B)** Accumulation of indium-111–labeled intact 7.16.4 mAb at the site of a neu-targeted vaccine and its draining lymph node. Administration of vaccine cells and antibodies was as same as in **A**. After 48 hours, VDLNs (left and right inguinal) and superficial cervical lymph nodes (used as a control for the non-draining lymph nodes) were isolated and their radioactivity was measured in a gamma counter. Plotted is the mean radioactivity (injection dose %) for 5 mice per group. *P* values comparing right and left inguinal lymph nodes were determined by Mann-Whitney *U* test.

complex is able of forming in vivo from an i.v. injection of the intact 7.16.4 mAb and a s.c. administration of the neu-targeted vaccine. The neu vaccine + antibody complex increased the uptake of vaccine cells by DCs and enhanced activation and proliferation of neu-specific CD8⁺ T cells in vivo in an Fc-dependent manner. These findings have important implications for the future development of combinatorial mAb + vaccine approaches for cancer therapy.

Results

The Fc portion is required for mAb-mediated enhancement of antitumor immunity. We have previously shown that coadministration of neu-targeted vaccine and neu-specific mAb enhances the antitumor response when compared with administration of vaccine or antibody alone (25). Moreover, CD4⁺ and CD8⁺ T cell depletion completely abrogates this response (27). Furthermore, although the intact 7.16.4 mAb mediates ADCC in vitro (data not shown), the depletion of NK cells using anti-asialo GM did not abrogate mAb enhancement of the vaccine-induced antitumor response in vivo (Supplemental Figure 1A; supplemental material available online with this article; doi:10.1172/JCI34333DS1). In addition, when clodronate liposomes were used to deplete phagocytes, the vaccine-induced antitumor response was significantly abrogated (Supplemental Figure 1B). To demonstrate whether the Fc portion of the mAb, which associates with FcγR and CRs present on phagocytes, in particular macrophages and DCs, is involved in antibody-mediated antitumor vaccine enhancement, we generated F(ab')₂ fragments of the intact 7.16.4 mAb for comparison with the activity of the intact 7.16.4 mAb. Enzymatic digestion of 7.16.4 was performed, and the generation of 7.16.4 F(ab')₂ was verified by Western blotting (data not shown). Specificity of the purified 7.16.4 F(ab')₂ for neu was verified by flow cytometric anal-

ysis of 7.16.4 F(ab')₂ and intact 7.16.4 mAb binding to NT2 cells using either an Fc-specific secondary antibody or a light-chain-specific secondary antibody to visualize binding (Figure 1A). Next, 7.16.4 F(ab')₂ and intact 7.16.4 mAb were compared in an in vivo study assessing tumor-free survival. Specifically, mice vaccinated with either the neu-expressing vaccine or mock vaccine also received either the intact 7.16.4 mAb or 7.16.4 F(ab')₂ and were challenged 2 weeks later with the NT tumor cells. As expected, coadministration of the intact antibody and neu-targeted vaccine resulted in a prolonged tumor-free survival and elimination of tumors in 60% of *neu-N* mice (Figure 1B). However, this treatment effect was not observed when 7.16.4 F(ab')₂ was used, even though the dose of 7.16.4 F(ab')₂ was 3-fold that of intact 7.16.4 mAb in these studies to account for the more rapid clearance of the F(ab')₂ molecule (Figure 1B). These data demonstrate a requirement for neu-specific intact IgG given concurrently with the vaccine in order to eliminate neu-expressing tumors in vaccinated animals. Because previous lymphocyte subset depletion experiments demonstrated that tumor elimination is CD8⁺ T cell dependent, we also examined the induction of neu-specific CD8⁺ T cells in vaccinated *neu-N* mice given either the intact 7.16.4 mAb or 7.16.4 F(ab')₂. In these studies, an ELISPOT assay was used to enumerate neu-specific CD8⁺ T cells directly isolated from tumor-bearing *neu-N* mice 14 days after vaccination. The highest proportion of neu-specific CD8⁺ T cells was found in mice treated with vaccine + intact 7.16.4 mAb (Figure 1C). In contrast, the neu-specific CD8⁺ T cell response in mice treated with vaccine + 7.16.4 F(ab')₂ was significantly lower than the response measured in intact 7.16.4 mAb–treated mice and was indistinguishable from vaccinated mice treated with control IgG. These data clearly show that coadministration of the intact mAb

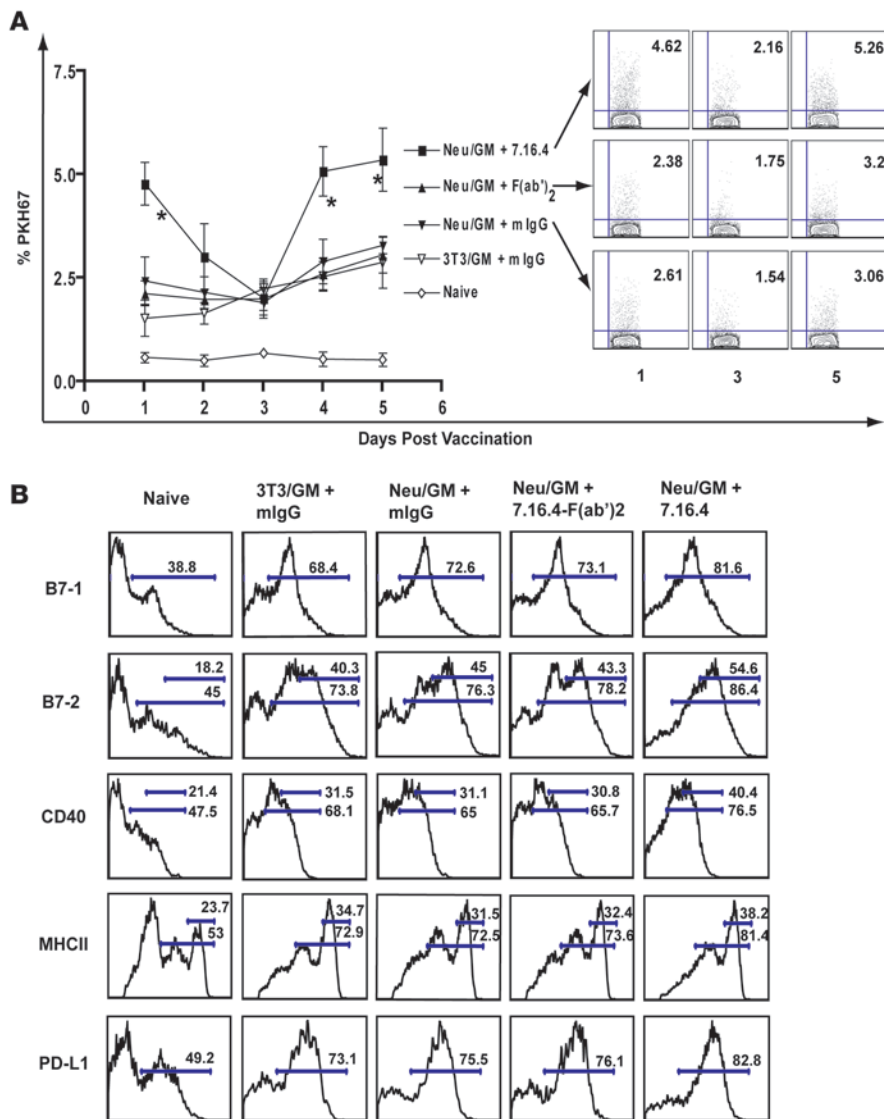


Figure 3

CD11c⁺ DCs take up vaccine cells most efficiently in mice treated with the neu-expressing, GM-CSF-secreting vaccine given concurrently with the intact 7.16.4 mAb. (A) neu-specific antibody increased the uptake of vaccine cells by CD11c⁺ DCs in an Fc-dependent manner. neu-targeted vaccine (3T3 neu/GM) or control vaccine (3T3/GM) cells were labeled with PKH67 and then injected s.c. (1×10^6 cells) into each limb of the mouse, followed by an i.p. injection of intact 7.16.4 mAb, 7.16.4 F(ab')₂, or a control IgG Ab. The VDLNs were harvested daily on days 1–5 following treatment, and DCs were isolated using the Miltenyi CD11c magnetic beads. Plotted are the mean percentages of PKH67-expressing CD11c⁺ DCs for 4–5 mice per group. A representative flow cytometric analysis is shown for the neu-targeted vaccine + intact 7.16.4 mAb, + 7.16.4 F(ab')₂, and + mIgG groups. **P* < 0.05 versus all other treatment groups, Mann-Whitney *U* test. The statistical analysis is shown in Table 1. (B) CD11c⁺ DCs isolated from the neu-targeted vaccine and intact 7.16.4 mAb-treated mice expressed higher levels of the maturation markers B7-1, B7-2, CD40, MHC-II, and PD-L1 when compared with CD11c⁺ DCs isolated from mice treated with the neu-targeted vaccine + 7.16.4 F(ab')₂ or + control antibody. Shown is a representative flow cytometric analysis of CD11c⁺ DCs isolated from 1 mouse per group. This experiment was repeated 3 times with similar results.

with neu-targeted vaccination results in an Fc-dependent augmentation of the tumor-specific CD8⁺ T cell responses that are associated with an increase in tumor-free survival.

Intact 7.16.4 mAb localizes at the site of neu vaccination. The administration of preformed antigen/antibody immune complex molecules is a commonly used method for enhancement of antigen-targeted cellular immunity by a mAb (28–31). However, less is known about antigen-antibody complex formation in vivo when the antibody is administered separately from the antigen. We therefore evaluated the ability of the intact 7.16.4 mAb to form immune complexes with the neu-targeted vaccine cells when each is delivered by separate routes of administration in vivo. In vivo SPECT/CT imaging was performed by administering indium-111-labeled 7.16.4 i.v. to neu-N mice concurrently with s.c. injected neu-expressing vaccine cells in the right leg and control vaccine cells in the left leg. Forty-eight hours later, a localized hot spot developed at the site of neu vaccination in the right leg (Figure 2A). A biodistribution study was conducted 48 hours after vaccination. Vaccine-draining lymph nodes (VDLNs) and superficial cervical lymph nodes (negative control) were excised, and their radioactivity content was mea-

sured. The right inguinal lymph node had approximately 4 times more radioactivity than the left inguinal lymph node (Figure 2B), suggesting that the neu-targeted mAb specifically bound to neu-expressing vaccine cells and formed complexes in the VDLN of the neu-targeted vaccine. In contrast, the indium-labeled control IgG-treated mice had no significant radioactivity accumulation in either lymph node (Figure 2B). Overall, both the in vivo SPECT/CT imaging and the biodistribution study data confirmed that the intact 7.16.4 mAb and neu-targeted vaccine cells were capable of forming immune complexes in vivo following different routes of administration of the antibody and the antigen. In addition, the in vivo complex formed by the neu-targeted mAb and the neu-expressing vaccine cells was antigen specific.

Intact 7.16.4 mAb enhances the in vivo uptake of neu vaccine cells by CD11c⁺ DCs in an Fc-dependent manner. The data presented so far show that the intact 7.16.4 mAb is able to aggregate specifically with the neu-targeted vaccine. This aggregate localizes in the draining lymph node 48 hours later. Since this aggregation appears to enhance the induction of neu-specific CD8⁺ T cells, we sought to determine the extent to which the in vivo localization of 7.16.4 to



Table 1

Percentage PKH67⁺CD11c⁺ DCs on days 1–5 after in vivo administration of vaccine + mAb

Treatment	% PKH67 ⁺ CD11c ⁺ DCs in VDLNs				
	Day 1	Day 2	Day 3	Day 4	Day 5
3T3 neu/GM + intact 7.16.4 mAb	4.78 ± 0.52	3.02 ± 0.80	2.02 ± 0.40	5.08 ± 0.60	5.36 ± 0.76
3T3 neu/GM + 7.16.4 F(ab') ₂	2.13 ± 0.3 ^A	1.98 ± 0.23	2.00 ± 0.28	2.61 ± 0.38 ^A	3.06 ± 0.44 ^A
3T3 neu/GM + mIgG	2.43 ± 0.57 ^A	2.15 ± 0.38	1.9 ± 0.36	2.90 ± 0.54 ^A	3.32 ± 0.23 ^A
3T3/GM + mIgG	1.53 ± 0.43 ^A	1.66 ± 0.26 ^A	2.25 ± 0.22	2.54 ± 0.36 ^A	2.88 ± 0.62 ^A
Naive	0.59 ± 0.12 ^A	0.51 ± 0.14 ^A	0.69 ± 0.06 ^A	0.55 ± 0.18 ^A	0.54 ± 0.16 ^A

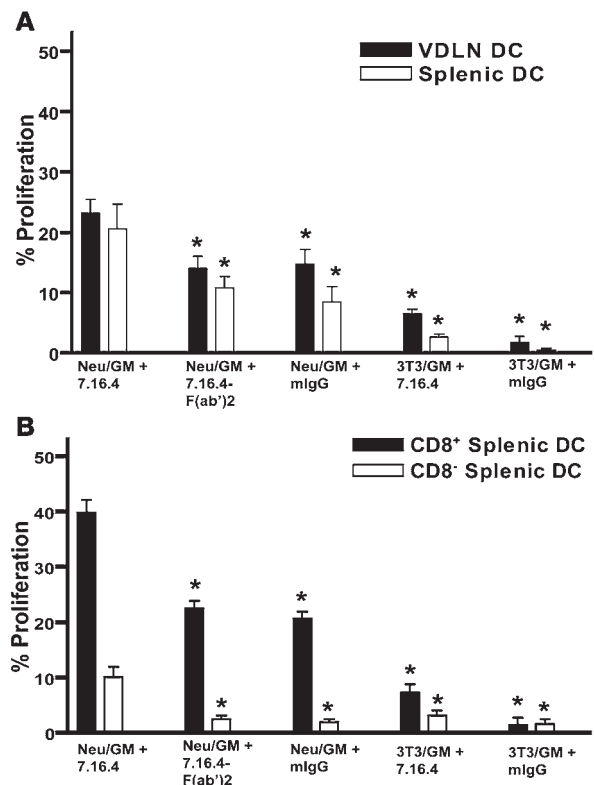
Data represent mean ± SD of at least triplicate samples. ^AP < 0.05 versus 3T3 neu/GM + intact 7.16.4 mAb, Mann-Whitney *U* test.

neu-targeted vaccine cells influences the in vivo uptake of the vaccine cells by lymph node CD11c⁺ DCs. neu vaccine or control vaccine cells were fluorescently labeled with PKH67, irradiated, and administered s.c., concurrently with i.p. injections of intact 7.16.4 mAb, 7.16.4 F(ab')₂, or control IgG Ab. The VDLNs were harvested each day from days 1 to 5. CD11c⁺ DCs were isolated from each group and analyzed for PKH67 expression by flow cytometry. PKH67⁺CD11c⁺ DCs were detected as early as 1 day after treatment, and the proportion of CD11c⁺ DCs that were PKH67⁺ was highest in the intact 7.16.4 mAb + neu-targeted vaccine group. In contrast, 7.16.4 F(ab')₂ administration did not result in increased uptake of vaccine cells compared with control IgG Ab (Figure 3A and Table 1). On days 2 and 3, the number of PKH67⁺CD11c⁺ DCs from the intact 7.16.4 mAb + neu-targeted vaccine treatment decreased to the level seen in the neu-targeted vaccine + 7.16.4 F(ab')₂ and + control IgG treatment. However, on days 4 and 5, the number of PKH67⁺CD11c⁺ DCs from the intact 7.16.4 mAb + neu-targeted vaccine treatment rebounded and again reached the highest level of all treatment groups (Figure 3A and Table 1). Fc-mediated phagocytosis is known to induce DC maturation. Therefore, the DC maturation markers B7-1, B7-2, CD40, MHC class II, and PD-L1 were evaluated 24–36 hours after treatment with the vaccination and either the intact 7.16.4 mAb or 7.16.4 F(ab')₂. As expected, the GM-CSF vaccine alone induced CD11c⁺ DC

maturation, as the control GM-CSF-secreting vaccine (3T3/GM) rapidly upregulated the expression of B7-1, B7-2, CD40, MHC-II, and PD-L1 on the CD11c⁺ DCs in the VDLN (Figure 3B). However, the intact 7.16.4 mAb enhanced the maturation of CD11c⁺ DCs above the expected GM-CSF maturation effect, as the lymph node CD11c⁺ DCs isolated from the mice that received the intact 7.16.4 mAb concurrently with the neu-targeted vaccine exhibited the highest expression levels of B7-1, B7-2, CD40, MHC-II, and PD-L1 (Figure 3B). In contrast, CD11c⁺ DCs isolated from mice treated with 7.16.4 F(ab')₂ and neu vaccine had maturation marker levels similar to those of mice treated with the neu vaccine and control IgG Ab. These data demonstrate that the Fc portion of 7.16.4 activates Fc-mediated phagocytosis in CD11c⁺ DCs to efficiently take up neu-targeted vaccine cells, consequently resulting in additional maturation of GM-CSF-stimulated CD11c⁺ DCs. Furthermore, these results provide additional evidence of the in vivo formation of immune complexes between the intact

Figure 4

CD11c⁺ DCs isolated from mice treated with the neu-expressing, GM-CSF-secreting vaccine given concurrently with intact 7.16.4 mAb induce efficient proliferation of naive neu-specific CD8⁺ T cells. (A) Naive RNEU_{420–429}-specific CD8⁺ T cells proliferated most vigorously in response to CD11c⁺ DCs isolated from mice treated with the neu-expressing, GM-CSF-secreting vaccine + intact 7.16.4 mAb. Administration of vaccine cells and antibodies was similar to that described in Figure 3A. On day 4 after vaccination, the spleen and VDLNs were harvested and DCs were isolated using the Miltenyi CD11c magnetic beads. Naive RNEU_{420–429}-specific CD8⁺ T cells were isolated, labeled with CFSE, and then cocultured with CD11c⁺-isolated DCs for 3 days. CFSE dilution was measured by flow cytometry. *n* = 5 mice per group. This analysis was repeated at least twice. (B) Both CD8⁺ and CD8⁻ DCs proliferated RNEU_{420–429}-specific CD8⁺ T cells most efficiently when the intact 7.16.4 mAb was administered with the neu-targeted vaccine. Administration of vaccine cells and antibodies was similar to that described in Figure 3A. On day 4, splenic CD11c⁺ DCs were isolated from each group, followed by FACS of CD8⁺ and CD8⁻ DCs. Subsequently, the DEAD assay was performed as described in A. *n* = 10 mice per group. This analysis was repeated at least twice. **P* < 0.05 versus intact 7.16.4 mAb + neu-targeted vaccine, Mann-Whitney *U* test.



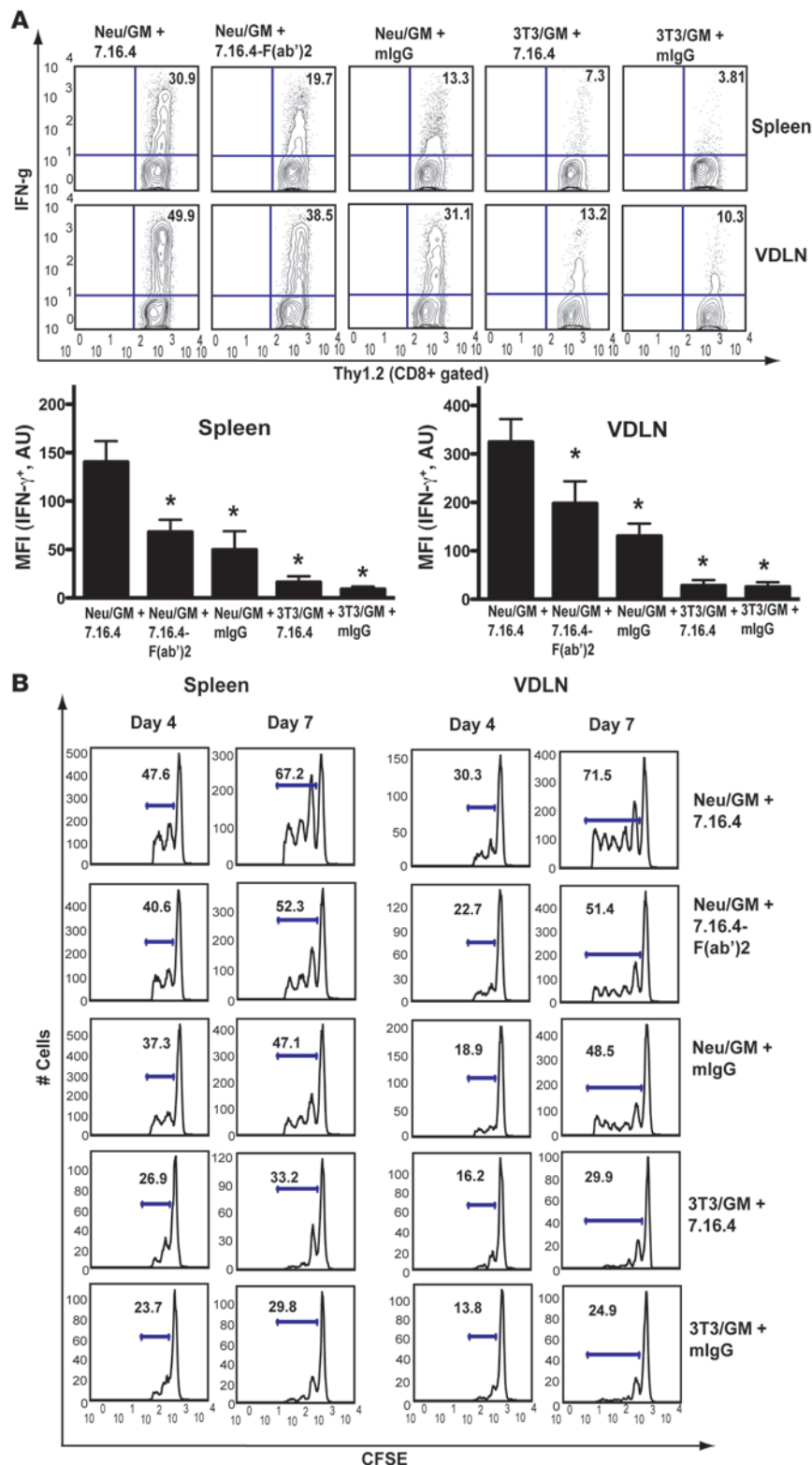


Figure 5

The neu-expressing, GM-CSF-secreting vaccine given concurrently with the intact 7.16.4 mAb enhances the effector function and proliferation capability of neu-specific CD8⁺ T cells *in vivo*. (A) The neu-expressing, GM-CSF-secreting vaccine given concurrently with the intact 7.16.4 mAb increases the number of activated IFN- γ -expressing RNEU₄₂₀₋₄₂₉-specific CD8⁺ T cells following treatment. Each *neu-N* mouse received 2×10^6 Thy1.2 RNEU₄₂₀₋₄₂₉-specific CD8⁺ T cells *i.v.*, followed by 1×10^6 3T3 neu/GM or 3T3/GM cells in each limb *s.c.* and intact 7.16.4 mAb (100 μ g), 7.16.4 F(ab')₂ (150 μ g), or irrelevant IgG (100 μ g) *i.p.* on day 0. Their spleens and VDLNs were harvested on day 4, and CD8⁺ T cells were isolated with the Miltenyi CD8a magnetic beads. The isolated CD8⁺ T cells were then cocultured (1×10^6) with RNEU₄₂₀₋₄₂₉-pulsed T2D^a (1×10^6) overnight. Thy1.2 RNEU₄₂₀₋₄₂₉-specific CD8⁺ T cells were stained for IFN- γ and analyzed by flow cytometry. The mean fluorescent intensity of IFN- γ in Thy1.2 RNEU₄₂₀₋₄₂₉-specific CD8⁺ T cells was also measured. Shown is a representative flow cytometric analysis for 1 mouse per group. This study was performed on a total of 3 mice per group per experiment and was repeated once. The statistical analysis is shown in Table 2. * $P < 0.05$ as determined by the Mann-Whitney *U* test compared with 3T3 neu/GM + intact 7.16.4 mAb group. (B) The intact 7.16.4 mAb enhances proliferation of adoptively transferred TCR transgenic T cells in vaccinated *neu-N* mice. CFSE dilution of Thy1.2 RNEU₄₂₀₋₄₂₉-specific CD8⁺ T cells was measured by flow cytometry. Shown is a representative flow cytometric analysis of 1 mouse per group. A total of 3 mice per group were analyzed per experiment, and this experiment was repeated once. The statistical analysis is shown in Table 3.

7.16.4 mAb and neu-targeted vaccine cells. Of note, the intact 7.16.4 mAb did not upregulate DC surface markers of maturation to a great extent (Figure 3B). In contrast, GM-CSF did increase all DC maturation markers (Figure 3B). Dhodapkar et al. (30) also reported that opsonization of cells did not extensively induce DC

maturation markers and that inflammatory cytokines such as GM-CSF were necessary for full DC maturation.

CD11c⁺ DCs isolated from neu-N mice treated concurrently with the intact 7.16.4 mAb + neu-targeted vaccine enhances the ex vivo proliferation of naive RNEU₄₂₀₋₄₂₉-specific CD8⁺ T cells. Because the intact



Table 2
Percentage IFN- γ -positive RNEU₄₂₀₋₄₂₉-specific CD8⁺ T cells 4 days after in vivo administration of vaccine + mAb

Treatment	% IFN- γ ⁺ clonotypic CD8 ⁺ T cells	
	Spleen	VDLN
3T3 neu/GM + intact 7.16.4 mAb	31.5 ± 3.7	48.3 ± 3.1
3T3 neu/GM + 7.16.4 F(ab') ₂	20.5 ± 2.8 ^A	37.2 ± 4.8 ^A
3T3 neu/GM + mIgG	15.1 ± 4.6 ^A	29.7 ± 4.2 ^A
3T3/GM + intact 7.16.4 mAb	8.11 ± 3.3 ^A	10.6 ± 1.8 ^A
3T3/GM + mIgG	3.44 ± 1.3 ^A	8.96 ± 1.0 ^A

Data represent mean ± SD of at least triplicate samples. ^AP < 0.05 versus 3T3 neu/GM + intact 7.16.4 mAb, Mann-Whitney U test.

7.16.4 mAb enhances the uptake of neu-targeted vaccine cells through Fc-mediated phagocytosis by CD11c⁺ DCs, we next performed a direct ex vivo antigen detection (DEAD) assay to assess whether this enhanced DC maturation effect results in enhanced DC cross-priming and induction of neu-specific CD8⁺ T cells. As a source of T cells, we used naive TCR transgenic CD8⁺ T cells specific for the immune-dominant neu epitope, RNEU₄₂₀₋₄₂₉ (32, 33). These T cells were stimulated in vitro with in vivo primed CD11c⁺ DCs. Lymph node CD11c⁺ DCs isolated on day 4 following treatment with the intact 7.16.4 mAb given concurrently with the neu-targeted vaccine induced the greatest proliferation of RNEU₄₂₀₋₄₂₉-specific CD8⁺ T cells (Figure 4A). Once again, the effect appeared to be Fc mediated, since the CD11c⁺ DCs isolated from mice given 7.16.4 F(ab')₂ + neu-targeted vaccine were unable to increase the proliferative capacity of the RNEU₄₂₀₋₄₂₉-specific CD8⁺ T cells above the neu-targeted vaccine-treated CD11c⁺ DC control group (Figure 4A). These results suggest that the intact 7.16.4 mAb given concurrently with the neu-targeted vaccine improves proliferation of neu-specific CD8⁺ T cells as a result of increased neu antigen presentation through enhanced uptake of neu-targeted vaccine cells by CD11c⁺ DCs in vivo.

Many studies have shown that DCs are the most capable of all APCs at effectively activating CD8⁺ T cells against an exogenous antigen because of their ability to constitutively cross-present the antigen to the endogenous antigen-processing pathway. However, one study suggested that the CD8⁻ DCs require activation via the Fc γ R or another signaling pathway to cross-present exogenous antigen (34). To evaluate whether the neu-targeted mAb enhances cross-presentation by one or both DC subtypes, CD11c⁺ DCs were separated into CD8⁺ DCs and CD8⁻ DCs, and these DC subsets were subsequently analyzed for their ability to induce proliferation of RNEU₄₂₀₋₄₂₉-specific CD8⁺ T cells. Our data show that even though CD8⁻ DCs isolated from mice treated only with neu-targeted vaccine were able to take up vaccine cells (data not shown), they were unable to proliferate RNEU₄₂₀₋₄₂₉-specific CD8⁺ T cells (Figure 4B). However, RNEU₄₂₀₋₄₂₉-specific CD8⁺ T cells proliferated to a significant extent when cultured with CD8⁻ DCs purified from mice treated with intact 7.16.4 mAb + neu-targeted vaccine. As expected, CD8⁺ DCs isolated from mice treated only with vaccine efficiently induced the proliferation of RNEU₄₂₀₋₄₂₉-specific CD8⁺ T cells without the need of Fc γ R activation. However, treatment with the vaccine + neu-targeted mAb further increased the cross-presentation capability of the CD8⁺ DCs (Figure 4B). Therefore, the capacity

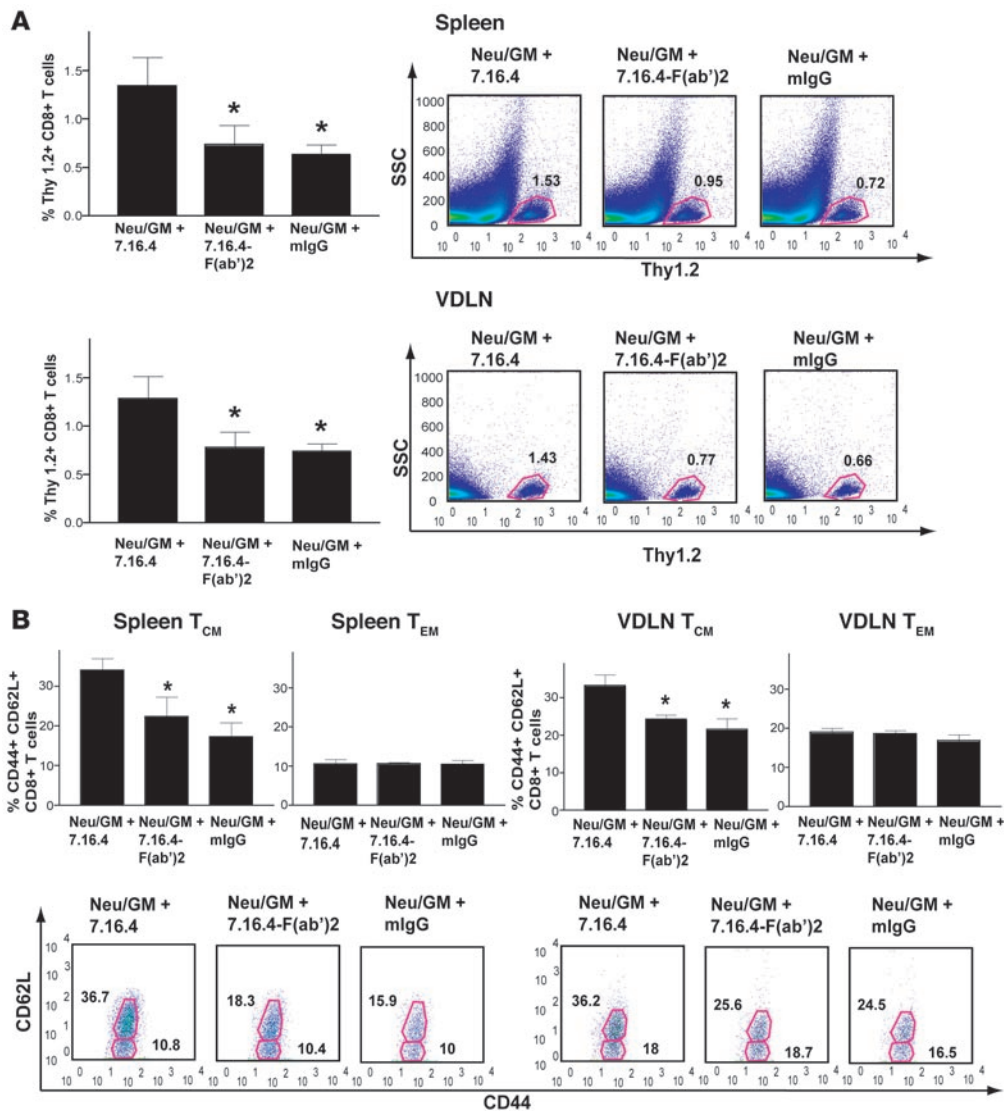
of CD8⁻ DCs to cross-prime appears dependent on the Fc portion of the intact 7.16.4 mAb, whereas CD8⁺ DCs do not appear to require the Fc portion for cross-priming but become more efficient at cross-priming if the antigen is taken up as immune complex. It is important to point out that both the CD8⁻ and CD8⁺ DCs stimulated a background level of proliferation of RNEU₄₂₀₋₄₂₉-specific CD8⁺ T cells (data not shown). We believe this background level was due to the uptake by DCs of endogenous circulating neu antigen in these neu-N mice that constitutively express the antigen in mammary tissue. In support of this hypothesis, we also isolated CD8⁺ and CD8⁻ DCs from untreated parental FVB mice, which do not constitutively express neu. Neither CD8⁺ nor CD8⁻ DCs from these untreated mice were able to induce any proliferation of naive RNEU₄₂₀₋₄₂₉-specific CD8⁺ T cells (data not shown). Finally, because CD8⁻ DCs have been shown to efficiently prime CD4⁺ T cells (35), we therefore sought to determine whether the intact 7.16.4 mAb had just as much of an influence on neu-specific CD4⁺ T cells as RNEU₄₂₀₋₄₂₉-specific CD8⁺ T cells. Interestingly, there was no difference in proliferation of neu-specific CD4⁺ T cells between neu-vaccinated mice that received the intact 7.16.4 mAb and those that were treated with the control IgG Ab (Supplemental Figure 2). This finding is in agreement with a study by Burgdorf et al. (36), in which MHC-II antigen presentation by DCs does not require the mannose receptor but rather depends on pinocytosis. Dudziak et al. (35) similarly suggest that the difference in the MHC-II antigen processing machinery in CD8⁺ and CD8⁻ DCs is intrinsically independent of surface markers and receptors.

Adoptively transferred RNEU₄₂₀₋₄₂₉-specific CD8⁺ T cells are activated and proliferate most extensively in neu-N mice treated concurrently with the intact 7.16.4 mAb and neu-targeted vaccine cells. To determine the extent to which the intact 7.16.4 mAb + neu-targeted vaccine treatment increases the effector function of neu-specific CD8⁺ T cells in vivo, we performed adoptive transfer experiments using Thy1.2⁻ RNEU₄₂₀₋₄₂₉-specific naive clonotypic CD8⁺ T cells isolated from TCR transgenic mice. Mice received clonotypic Thy1.2⁺ T cells i.v.,

Table 3
Percentage proliferation of RNEU₄₂₀₋₄₂₉-specific CD8⁺ T cells 4 and 7 days after in vivo administration of vaccine + mAb

Treatment	% Proliferation of clonotypic CD8 ⁺ T cells	
	Spleen	VDLN
Day 4		
3T3 neu/GM + intact 7.16.4 mAb	47.7 ± 2.6	31.2 ± 2.5
3T3 neu/GM + 7.16.4 F(ab') ₂	41.8 ± 1.7 ^A	21.3 ± 3.2 ^A
3T3 neu/GM + mIgG	38.7 ± 3.5 ^A	20.0 ± 2.1 ^A
3T3/GM + intact 7.16.4 mAb	28.8 ± 2.3 ^A	17.1 ± 3.8 ^A
3T3/GM + mIgG	26.5 ± 5.0 ^A	15.3 ± 1.8 ^A
Day 7		
3T3 neu/GM + intact 7.16.4 mAb	68.3 ± 3.8	71.5 ± 3.4
3T3 neu/GM + 7.16.4 F(ab') ₂	51.4 ± 5.3 ^A	53.0 ± 4.7 ^A
3T3 neu/GM + mIgG	47.8 ± 3.1 ^A	47.1 ± 4.3 ^A
3T3/GM + intact 7.16.4 mAb	31.4 ± 1.9 ^A	28.2 ± 3.9 ^A
3T3/GM + mIgG	28.7 ± 3.3 ^A	26.0 ± 3.8 ^A

Data represent mean ± SD of at least triplicate samples. ^AP < 0.05 versus 3T3 neu/GM + intact 7.16.4 mAb, Mann-Whitney U test.

**Figure 6**

A neu-expressing, GM-CSF-secreting vaccine given concurrently with the intact 7.16.4 mAb promotes the development of RNEU₄₂₀₋₄₂₉-specific CD8⁺ T_{CM}. (A) The intact 7.16.4 mAb increases the total population of RNEU₄₂₀₋₄₂₉-specific CD8⁺ T cells with time. Each *neu-N* mouse received the same treatment protocol as described in Figure 5A, except 4×10^6 Thy1.2⁺ RNEU₄₂₀₋₄₂₉-specific CD8⁺ T cells were used instead of 2×10^6 cells. After 30 days, the mice were boosted with 1×10^6 3T3 neu/GM cells in all 4 limbs. One week after the boost, their spleens and VDLNs were harvested and CD8⁺ T cells were isolated using the Miltenyi CD8a magnetic beads. The proportion of Thy1.2⁺ RNEU₄₂₀₋₄₂₉-specific CD8⁺ T cells present in the isolated CD8⁺ T cell population was analyzed by flow cytometry. (B) The intact 7.16.4 mAb enhances proliferation of RNEU₄₂₀₋₄₂₉-specific CD8⁺ T_{CM}. Thy1.2⁺ RNEU₄₂₀₋₄₂₉-specific CD8⁺ T cells from the experiment described in A were stained for CD62L and CD44 and analyzed by flow cytometry. Shown is a representative flow cytometric analysis of 1 mouse per group. A total of 3 mice per group were analyzed, and this study was repeated once. The gating represents Thy1.2⁺ CD8⁺ T cells. * $P < 0.05$ versus intact 7.16.4 mAb + neu-targeted vaccine, Mann-Whitney *U* test.

vaccine s.c., and mAb i.p. on day 0. To measure their activation state, we isolated CD8⁺ T cells from the treatment groups on day 4 following vaccination. Isolated CD8⁺ T cells were cultured with T2D⁹ cells pulsed with RNEU₄₂₀₋₄₂₉ overnight and then stained with mAbs against Thy1.2 and intracellular IFN- γ . In the spleen and VDLNs on day 4, CD8⁺ T cells from mice treated with the intact 7.16.4 mAb + neu-targeted vaccine demonstrated the highest proportion of Thy1.2⁺ RNEU₄₂₀₋₄₂₉-specific CD8⁺ T cells that both were positive for intracellular IFN- γ and exhibited the highest mean fluorescent intensity (Figure 5A and Table 2). In addition,

the coadministration of the intact 7.16.4 mAb + neu-targeted vaccine cells significantly increased the proliferation of Thy1.2⁺ RNEU₄₂₀₋₄₂₉-specific CD8⁺ T cells when compared with the neu-targeted vaccine given with either 7.16.4 F(ab')₂ or control IgG Ab (Figure 5B and Table 3). These data further support the role of the Fc portion of 7.16.4 as being the mediator of enhanced activation and proliferation of neu-specific CD8⁺ T cells.

Adoptively transferred RNEU₄₂₀₋₄₂₉-specific CD8⁺ T cells most effectively develop into central memory cells in neu-N mice treated with the intact 7.16.4 mAb and neu-targeted vaccine cells. The main purpose of vacci-



nation is to generate memory T cells that can provide long-lasting protection against diseases that express disease-specific antigens. Thus, we sought to determine the extent to which the neu-specific intact mAb given with the neu-targeted vaccine generates neu-specific memory CD8⁺ T cells. The adoptive transfer experiment was carried out as described in Figure 5A. After 30 days, the mice were boosted with neu-targeted vaccine cells. A week after the boost, the mice that had received the intact 7.16.4 mAb + neu-targeted vaccine treatment had the highest population of Thy1.2⁻ RNEU₄₂₀₋₄₂₉-specific CD8⁺ T cells in both the spleen and VDLNs (Figure 6A). Memory CD8⁺ T cells express CD44⁺ and are categorized as central (T_{CM}) or effector memory (T_{EM}) cells based on CD62L expression (33). The proportion of CD44⁺ cells that were also CD62L⁺, indicating T_{CM} phenotype, was highest in both the spleen and VDLNs from mice that received the intact 7.16.4 mAb + neu-targeted vaccine treatment (Figure 6B). However, the proportion of CD44⁺ CD62L⁻ T_{EM} remained at a similar level in all treatment groups (Figure 6B). These data demonstrate that the intact 7.16.4 mAb given with the neu-targeted vaccine enhances T_{CM} development compared with vaccine given alone or with the Fc-deficient neu-targeted mAb.

Discussion

To our knowledge, this is the first report demonstrating the trafficking and uptake by CD11c⁺ DCs of in vivo-formed tumor antigen-tumor mAb immune complexes. The data reported here reveal 2 findings that elucidate an important mechanism by which a neu-targeted mAb enhances the induction and activation of a potent immune response to a neu-targeted vaccine given concurrently. First, we show that the intact 7.16.4 mAb enhances vaccine-mediated antitumor CD8⁺ T cell activation and tumor elimination by an Fc-dependent mechanism. Second, we demonstrate that the coadministration of the intact 7.16.4 mAb and neu-targeted vaccine increases the uptake of vaccine cells by CD11c⁺ DCs, thereby enhancing activation, proliferation, and T_{CM} development of neu-specific CD8⁺ T cells. Taken together, these data provide results of a comprehensive ex vivo and in vivo analysis of one mechanism by which a tumor antigen-specific mAb can synergize with a vaccine targeting the same tumor antigen to enhance the overall systemic antitumor response.

Our neu-targeted vaccine cells secrete GM-CSF, which is a potent activator and recruiter of DCs. Based on the finding that the FcγR is required to mediate the 7.16.4-enhanced antitumor response, we evaluated the role of CD11c⁺ DCs in enhancing the antibody-mediated antitumor response, since CD11c⁺ DCs express FcγRs and serve as a bridge to the adaptive immune system. Several studies have shown that the administration of antibodies bound to antigens prior to in vivo administration can enhance the activation of antigen-specific CD8⁺ T cells (28–31). However, in the case of a GM-CSF-secreting vaccine approach that aims to attract and mature DCs at the vaccine site, the administration of immune-complexed vaccine cells would be expected to be less effective, as they may not secrete GM-CSF properly due to opsonization and would be readily taken up by CD11c⁺ DCs directly via the FcγR. In addition, a precomplexed vaccine would not be expected to involve DCs in priming CD8⁺ T cells, since they would require 2–4 days to be exposed to the tumor antigen and matured prior to activation of CD8⁺ T cells (13). Therefore, we reasoned that the enhanced antitumor response of the antibody-vaccine complex was likely due to concurrent

administration by different routes of delivery, thereby allowing gradual formation of the immune complex and prolonged secretion of GM-CSF up to a concentration level that is sufficient to effectively increase production and recruitment of DCs. Our biodistribution and in vivo imaging data support this concept and show that a strong localization of the intact 7.16.4 mAb at the vaccine site is not apparent until 48 hours following administration. In addition, our in vivo antigen uptake results indicate that CD11c⁺ DCs in VDLNs do not increasingly take up immune-complexed vaccine cells until 3 days after coadministration. These findings validate our group's prior observations demonstrating that a GM-CSF vaccine recruits DCs in vivo to the tumor site, which then traffic over days to the VDLN and ultimately activate both CD4⁺ and CD8⁺ T cells. These findings also provide support for an additional mechanism by which an antigen-targeted mAb synergistically enhances the induction of antigen-specific CD8⁺ T cells by the GM-CSF-secreting vaccine.

DCs gain their function of antigen presentation upon maturation, for which phagocytosis provides a strong stimulus (25). Because the intact 7.16.4 mAb + neu-targeted vaccine treatment increased the vaccine cell uptake, it resulted in an additional increase in the expression levels of GM-CSF-induced DC maturation markers. Consequently, CD11c⁺ DCs from the mAb + vaccine treatment enhanced the proliferation of RNEU₄₂₀₋₄₂₉-specific CD8⁺ T cells ex vivo. It has been shown that CD8⁺ DCs are inherently efficient at cross-presentation even without FcγRs, whereas the capacity of CD8⁺ DCs to present exogenous antigens on MHC class I molecules requires activation of FcγRs (34). Akiyama et al. (37) have shown that IgG-complexed apoptotic tumor cells (ATC-ICs) significantly enhanced phagocytosis by, and maturation of, CD8⁺ DCs in vitro and have demonstrated that CD8⁺ DCs loaded with ATC-ICs improved the antitumor response in their mouse model. Our data show similar findings. CD8⁺ DCs from the neu-targeted vaccine + either control IgG or 7.16.4 F(ab')₂ treatment failed to proliferate RNEU₄₂₀₋₄₂₉-specific CD8⁺ T cells. However, when the intact 7.16.4 mAb was used, RNEU₄₂₀₋₄₂₉-specific CD8⁺ T cells proliferated extensively following stimulation by CD8⁺ DCs. Therefore, in our study, the intact 7.16.4 mAb likely enhances phagocytosis of irradiated, and therefore apoptotic, vaccine cells and induces cross-presentation of neu by CD8⁺ DCs. This also may be the primary reason for the enhanced proliferation of adoptively transferred RNEU₄₂₀₋₄₂₉-specific CD8⁺ T cells in *neu-N* mice. It is noteworthy to mention that while murine DCs express high levels of CD8, none of the human DC subpopulations have been shown to express the CD8 marker (38). However, Dhodapkar et al. (30) have shown that human DCs also have the ability to enhance their cross-presentation of tumor cellular antigens through an FcγR-dependent mechanism.

Although the DEAD assay gives an ex vivo account of the direct interaction between CD11c⁺ DCs and RNEU₄₂₀₋₄₂₉-specific CD8⁺ T cells, the adoptive transfer of RNEU₄₂₀₋₄₂₉-specific CD8⁺ T cells into *neu-N* mice provides a unique assessment of the antigen-specific CD8⁺ T cell population influenced by the antibody in vivo. Adoptively transferred RNEU₄₂₀₋₄₂₉-specific CD8⁺ T cells were activated and proliferated most extensively in the group that received the intact 7.16.4 mAb and neu-targeted vaccine. In addition, a vaccine and antibody boost enhanced the development of T_{CM} more efficiently in the intact mAb-treated mice. The mAb-induced enhancement of T_{CM} development is significant because T_{CM} cells have access to secondary lymphoid



organs and can be activated by mature DCs, whereas T_{EM} cells are mainly excluded from these areas and are stimulated by nonprofessional APCs (39). It is therefore not surprising that in our study the proportion of T_{EM} cells after the boost was similar among all treatment groups. Because the T_{EM} cells sampled were from the spleen and lymph nodes, we may have missed evaluating the majority of T_{EM} cells that reside outside of these secondary lymphoid organs. Therefore, our analysis on T_{EM} cells is most likely only a partial view of the extent to which the neu-targeted mAb given concurrently with the neu-targeted vaccine influences T_{EM} development.

It is interesting to note that the $CD8^+$ T cell activation and proliferation measured in the spleen was higher than expected when the intact 7.16.4 mAb was given with vaccine, even though the in vivo imaging studies demonstrated localization in the VDLN with minimal uptake in the spleen. This observation could be due to the endogenous neu in our transgenic model, but the relatively low background level from the intact 7.16.4 mAb + control vaccine treatment would suggest otherwise. Although DC activity mainly takes place in the draining lymph node, systemic distribution of DCs that carry locally administered antigens has been observed under certain conditions (40–42). In our DEAD assay experiments, $CD11c^+$ DCs in the spleen proliferated naive clonotypic $CD8^+$ T cells just as well as those in VDLNs. Furthermore, the intact 7.16.4 mAb + neu-targeted vaccine treatment enhanced the cross-priming capabilities of splenic $CD8^+$ and $CD8^-$ DCs. We believe that DCs in a systemic GM-CSF milieu, created by the neu-targeted vaccine, are capable of migrating from the vaccine site to other organs such as the spleen, hence leading to the amplification of T cell functions at those sites. Additional studies are needed to elucidate the migratory pattern of DCs in a GM-CSF circulatory environment, starting with the in vivo imaging of vaccinated mice beyond the 48-hour time period.

This study provides what we believe to be the first in-depth analysis tracking over time the in vivo kinetics of an antigen-targeted mAb and vaccine given concurrently. We previously reported that a 14-day time period was required to achieve optimal activation of antigen-specific $CD8^+$ T cells following our GM-CSF vaccine approach (13). Additional studies provided evidence that a number of days were required for DC activation and trafficking to lymph nodes prior to the activation of T cells (13). However, less was known about the kinetics of the vaccine when given in combination with an antigen-targeted mAb. The in vivo radiolabeled vaccine analyses clearly show the direct interaction of the mAb with the neu-expressing vaccine cells and that this interaction reaches its peak at about 48 hours after coadministration. Furthermore, these studies directly show the rate of uptake of tumor-antibody complexes by $CD11c^+$ DCs attracted to the tumor site via GM-CSF secretion. In addition, these studies reveal the time it takes for $CD11c^+$ DCs to traffic to the VDLN for priming of T cells. Finally, and perhaps most importantly, the data demonstrate that the neu-targeted vaccine given with neu-specific mAb improves development of T_{CM} , which can be activated upon encountering neu-overexpressing tumor cells and neu antigen-presenting DCs.

Other preclinical studies have shown that similar neu-targeted antibodies can induce tumor killing through an NK-mediated ADCC mechanism (16, 43). It is important to point out that the original therapeutic intention of neu-targeted antibody-based immunotherapy was to inhibit unregulated proliferative and

antiapoptotic signaling pathways in tumor cells. In a recent clinical study on trastuzumab (which is a human analog of 7.16.4) monotherapy, Mohsin et al. (15) showed that in primary breast cancer, trastuzumab treatment results in tumor regression mainly through inhibition of PI3K/Akt pathways and subsequent induction of apoptosis rather than through retardation of cell proliferation. So far, there is no evidence of trastuzumab's ability to direct immunomodulatory functions in humans. However, tumors create a microenvironment, which suppresses the function of immune effector cells that are essential for tumor recognition and eradication. This could be one reason we have yet to see trastuzumab's immunomodulatory effects in the clinical setting.

In conclusion, our study provides an extensive ex vivo and in vivo analysis of an Fc-mediated mechanism by which an antigen-specific mAb enhances a $CD8^+$ T cell immune response induced by a vaccine targeted against the same tumor antigen in immune-tolerant mice. This mechanism requires $CD11c^+$ DCs and results in the enhanced activation and proliferation of $CD8^+$ T cells and ultimately the enhanced generation of T_{CM} . The tumor microenvironment has the capability to inhibit the therapeutic potential of immune-based therapies by suppressing the development of DCs and increasing the generation of Tregs, which in turn suppress effector T cells. Thus, interventions that target the same antigen in multiple ways may be one approach to overcoming the multiple mechanisms involved in downregulating T cell function within the tumor's microenvironment. Successful immune-based therapies will ultimately require the combination of agents that target tumor antigens and agents that inhibit the multiple pathways involved in downregulating T cells specific for these antigens.

Methods

Animals and cell lines. The *neu-N* mice (line N 202) (44) were obtained from W. Muller (McMaster University, Hamilton, Ontario, Canada). Animals were kept in pathogen-free conditions and were treated in accordance with institutional and American Association of Laboratory Animal Committee policies. All animal studies were approved by the institutional review board of Johns Hopkins University. The cell lines 3T3/GM (mock vaccine) and 3T3 neu/GM (vaccine) are 3T3 cells that have been genetically modified to express the *GM-CSF* gene and the *GM-CSF* and *HER-2/neu* genes, respectively. The NT2 cells are transplantable neu-expressing mammary tumor cells derived from a spontaneous mammary tumor that formed in a *neu-N* mouse. Both vaccine and tumor lines have been previously described (45). NT2/B7-1 cells are NT2 cells transduced with a human B7-1-encoding retrovirus, as described previously (13). The 3T3 NP/GM cells are 3T3/GM cells engineered to express lymphocytic choriomeningitis virus NP under the selection with hygromycin B at 150 μ g/ml (Roche Diagnostics).

mAbs. Hybridoma expressing the murine and anti-rat neu-specific 7.16.4 (IgG2a) mAb was obtained from M. Greene (University of Pennsylvania, Philadelphia, Pennsylvania, USA). Through a protein G column, the intact 7.16.4 mAb was purified from ascites that were prepared by Harlan Bioproducts for Science Inc. The $F(ab')_2$ fragment of 7.16.4 was generated using the ImmunoPure $F(ab')_2$ Preparation Kit (Pierce Biotechnology). FITC-conjugated anti-mouse Fc-specific antibody (Sigma-Aldrich) and FITC-conjugated anti-mouse Ig λ_1 , λ_2 , and λ_3 light chain antibody (BD Biosciences – Pharmingen) were used to confirm the $F(ab')_2$ fragment binding to neu. Ab-3 (EMD Biosciences), which recognizes an intracellular epitope of neu, was used to visualize western-blotted neu for the internalization studies. mAbs against $CD11c$, $CD80$, $CD86$, $CD40$, MHC-II, IFN- γ , $CD62L$, and PD-L1 (B7-H1) were purchased from BD Biosciences.



Tumor prevention experiment. Eight-week-old female *neu-N* mice were vaccinated with 1×10^6 3T3 neu/GM cells or with 1×10^6 3T3 NP/GM cells as a control, followed 2 weeks later by s.c. tumor challenge with 2×10^5 cells, as previously described (46). Animals then received i.p. injections of neu-specific intact mAb, F(ab')₂ fragment or control polyclonal mouse IgG (mIgG; Sigma-Aldrich) on the day of the tumor challenge. All antibody preparations were sterile filtered (0.22-mm pore size mStar filters, Costar; Corning) before injection. The intact and control antibodies were administered weekly for a total of 5 injections (100 µg of IgG per injection) thereafter. The F(ab')₂ fragment was injected twice per week for a total of 10 injections [150 µg of F(ab')₂ per injection] due to its higher clearance rate. Animals were monitored twice per week for palpable tumors.

ELISPOT assays. Eight-week-old female *neu-N* mice were given either neu-targeted vaccine or control vaccine on day -14 and an NT2 challenge (2×10^5 cells) on day 0. On the day of tumor challenge, animals began receiving weekly injection of 100 µg of control IgG, 100 µg of 7.16.4, or 300 µg of 7.16.4 F(ab')₂. The amount of 7.16.4 F(ab')₂ was determined by taking into the account the F(ab')₂ fragment's high clearance rate and adjusting for molar equivalency. After 14 days, the mice were sacrificed, and spleens were harvested. neu-specific CD8⁺ T cells were quantified by ELISPOT analysis as previously described with modifications (47). Splenocytes were briefly treated with ACK Lysis Buffer (Quality Biological Inc.) for red blood cell lysis, and CD8⁺ T cells were negatively selected using the Dynal Mouse CD8 Negative Isolation Kit (Dynal Biotech). neu-expressing target cells, NT2/B7-1, were pretreated for 2 days with IFN-γ to upregulate MHC-I on their surface. ELISPOT analysis for IFN-γ production was performed using the murine IFN-γ ELISPOT Kit (R&D Biosystems). Isolated CD8⁺ T cells were incubated with NT2/B7-1 target cells overnight at 37°C and 5% CO₂ at an effector/target ratio of 10:1 (10^5 CD8⁺ T cells, 10^4 NT2/B7-1 cells). The ELISPOT plates were developed according to the manufacturer's instructions. CD8⁺ T cells and NT2/B7-1 cells alone were used as controls. Spots were counted using the KS ELISPOT scope and software (Zeiss). The number of spots formed in control wells (CD8⁺ T cells alone) were averaged and subtracted from the number of spots in each well with CD8⁺ T cells plus targets.

Biodistribution study and in vivo imaging. For the biodistribution study, 8-week-old, female *neu-N* mice were given 3T3 neu/GM (1×10^6 cells) in the right leg and 3T3 NP/GM (1×10^6 cells) in the left leg s.c., followed by i.v. injection of 100 µg of radiolabeled indium-111 7.16.4 or 100 µg of radiolabeled indium-111 control IgG. The antibody was radiolabeled using methodology described previously (48, 49). After 48 hours, lymph nodes were excised. The right and left inguinal lymph nodes were used as the VDLNs, and the superficial cervical lymph node was used as the baseline control. The lymph nodes were placed in a gamma counter to measure their radioactivity.

The initial set up for the in vivo imaging was similar to the biodistribution study. After s.c. administration of the vaccine cells (3T3 neu/GM [1×10^6 cells] in the right leg and 3T3 NP/GM [1×10^6 cells] in the left leg) and the radiolabeled 7.16.4 (100 µg), the mice were anesthetized with 3% isoflurane, maintained at 1%–2% afterward with a constant oxygen flow rate of 1 l/min. SPECT/CT images were taken at 1, 24, and 48 hours after injection on an XSPECT system with a pinhole collimator for indium-111 photons (GammaMedica).

In vivo uptake of vaccine cells. We labeled 2×10^7 3T3 neu/GM or 3T3/GM cells per ml with the green fluorescent cell linker dye PKH67 (4×10^{-6} M) according to the manufacturer's instructions (Sigma-Aldrich), and then 1×10^6 cells of either vaccine line were irradiated and then injected s.c. into each of the 4 limbs of an 8-week old female FVB/N mouse, followed by i.p. injection of the intact 7.16.4 mAb (100 µg), 7.16.4 F(ab')₂ (300 µg), or control mIgG (100 µg) mAbs. From days 1 through 5, VDLNs (axillary,

brachial, and inguinal) were harvested and DCs were isolated with CD11c magnetic beads (Miltenyi Biotec). The amount of PKH67⁺CD11c⁺ DCs was determined by flow cytometry.

DEAD assay. Eight-week old female *neu-N* mice were given vaccine cells and antibodies as described above. On day 4, VDLNs (axillary, brachial, and inguinal) and spleens were harvested, and lymph node and splenic DCs were isolated using CD11c magnetic beads (Miltenyi Biotec). Cell sorting was performed to purify CD8⁺ and CD8⁻ DC subsets from splenic CD11c⁺ DCs, as described by den Haan and Bevan (34). Isolated or purified CD11c⁺ DCs were cultured in a 96-well U-bottom plate with clonotypic Thy 1.2 CD8⁺ T cells from a TCR transgenic mouse. These clonotypic CD8⁺ T cells, which are specific for the immunodominant neu epitope containing amino acids 420–429 (RNEU_{420–429}) (32, 33), were isolated using the Dynal CD8 Negative Isolation Kit (Dynal Biotech) and were then labeled with CFSE (Invitrogen). The effector (RNEU_{420–429}-specific T cells) to target (CD11c⁺ DCs or CD8⁻ DCs) ratio was 3:1 (7.5×10^5 cells/ 2.5×10^5 cells). Because the CD8⁺ DC population is significantly less than CD8⁻ DCs, the effector/target ratio of 1.5×10^6 CD8⁺ DCs/ 5×10^4 RNEU_{420–429}-specific CD8⁺ T cells was used. On day 3, CFSE dilution of RNEU_{420–429}-specific T cells was measured by flow cytometry.

Adoptive transfer experiments. For the in vivo proliferation study, 2×10^6 CFSE-labeled Thy1.2 RNEU_{420–429}-specific CD8⁺ T cells were adoptively transferred i.v. into 8-week old female *neu-N* mice, followed by administration of 3T3 neu/GM (1×10^6 per limb) or 3T3 GM (1×10^6 per limb) s.c. and the intact 7.16.4 mAb (100 µg), 7.16.4 F(ab')₂ (300 µg), or control mIgG mAb (100 µg) i.p. On days 4 and 7, VDLNs (axillary, brachial, and inguinal) and spleens were harvested. CD8⁺ T cells were isolated using CD8a magnetic beads (Miltenyi Biotec). CFSE dilution of the adoptively transferred Thy1.2 RNEU_{420–429}-specific CD8⁺ T cells was measured by flow cytometry. In addition, the isolated CD8⁺ T cells (1×10^6) on day 4 were cocultured with RNEU_{420–429}-pulsed T2D^a (1×10^6) overnight and then stained for IFN-γ. Thy1.2 RNEU_{420–429}-specific CD8⁺ T cells positive for IFN-γ were analyzed by flow cytometry. To analyze Thy1.2 RNEU_{420–429}-specific memory CD8⁺ T cells, 4×10^6 of these clonotypic CD8⁺ T cells were adoptively transferred i.v., followed by administration of vaccine cells and antibodies as described above. After 30 days, the mice were boosted with 3T3 neu/GM (1×10^6 per limb) or 3T3/GM (1×10^6 per limb) s.c. One week later, VDLNs (axillary, brachial, and inguinal) and spleens were harvested and analyzed for expression of CD62L by flow cytometry.

Statistics. The Mann-Whitney *U* test was used to analyze ELISPOT data. Log-rank tests were used to analyze tumor-free survival and compare treatment groups. *P* < 0.05 was considered statistically significant. The GraphPad Prism3 Program (GraphPad Software) was used to perform all statistical analyses. In all figures, error bars represent SD.

Acknowledgments

We gratefully acknowledge Lee Blosser and Ada Tam at the Flow Cytometry Core Facility at the Johns Hopkins University School of Medicine for their expert technical help with CD8⁺ and CD8⁻ DC cell sorting. We thank Mark Greene at the University of Pennsylvania for generously providing the intact 7.16.4 mAbs.

Received for publication October 24, 2007, and accepted in revised form February 20, 2008.

Address correspondence to: Peter S. Kim, Johns Hopkins University School of Medicine, 1650 Orleans Street, CRB1 4M86, Baltimore, Maryland 21231, USA. Phone: (443) 690-4129; Fax: (410) 614-8216; E-mail: pskim07@gmail.com.



1. Gallegos, A.M., and Bevan, M.J. 2006. Central tolerance: good but imperfect. *Immunol. Rev.* **209**:290–296.
2. Li, L., and Boussiotis, V.A. 2006. Physiologic regulation of central and peripheral T cell tolerance: lessons for therapeutic applications. *J. Mol. Med.* **84**:887–899.
3. Piccirillo, C.A., and Shevach, E.M. 2004. Naturally-occurring CD4⁺CD25⁺ immunoregulatory T cells: central players in the arena of peripheral tolerance. *Semin. Immunol.* **16**:81–88.
4. Wang, H.Y., and Wang, R.F. 2007. Regulatory T cells and cancer. *Curr. Opin. Immunol.* **19**:217–223.
5. Drake, C.G., Jaffee, E., and Pardoll, D.M. 2006. Mechanism of immune evasion by tumors. *Adv. Immunol.* **90**:51–81.
6. Gajewski, T.F., et al. 2006. Immune resistance orchestrated by the tumor microenvironment. *Immunol. Rev.* **213**:131–145.
7. Emens, L.A., and Jaffee, E.M. 2005. Leveraging the activity of tumor vaccines with cytotoxic chemotherapy. *Cancer Res.* **65**:8059–8064.
8. Kim, R., Emi, M., and Tanabe, K. 2005. Cancer cells immune escape and tumor progression by exploitation of anti-inflammatory and pro-inflammatory responses. *Cancer Biol. Ther.* **4**:924–933.
9. Kusmartsev, S., Nefedova, Y., Yoder, D., and Gabrilovich, D.I. 2004. Antigen-specific inhibition of CD8⁺ T cell response by immature myeloid cells in cancer is mediated by reactive oxygen species. *J. Immunol.* **172**:989–999.
10. Kusmartsev, S., and Gabrilovich, D.I. 2006. Role of immature myeloid cells in mechanisms of immune evasion in cancer. *Cancer Immunol. Immunother.* **55**:237–245.
11. Balkwill, F., Charles, K.A., and Mantovani, A. 2005. Smoldering and polarized inflammation in the initiation and promotion of malignant disease. *Cancer Cell.* **7**:211–217.
12. Laheru, D.A., Pardoll, D.M., and Jaffee, E.M. 2005. Genes to vaccines for immunotherapy: how the molecular biology revolution has influenced cancer immunology. *Mol. Cancer Ther.* **4**:1645–1652.
13. Dranoff, G., et al. 1993. Vaccination with irradiated tumor cells engineered to secrete murine GM-CSF stimulates potent, specific, long lasting antitumor immunity. *Proc. Natl. Acad. Sci. U. S. A.* **90**:3539–3543.
14. O'Mahony, D., and Bishop, M.R. 2006. Monoclonal antibody therapy. *Front. Biosci.* **11**:1620–1635.
15. Mohsin, S.K., et al. 2005. Neoadjuvant trastuzumab induces apoptosis in primary breast cancers. *J. Clin. Oncol.* **23**:2460–2468.
16. Clynes, R.A., Towers, T.L., Presta, L.G., and Ravetch, J.V. 2000. Inhibitory Fc receptors modulate in vivo cytotoxicity against tumor targets. *Nat. Med.* **6**:443–446.
17. Cartron, G., et al. 2002. Therapeutic activity of humanized anti-CD20 monoclonal antibody and polymorphism in IgG Fc receptor FcγRIIIa gene. *Blood.* **99**:754–758.
18. Weng, W.K., and Levy, R. 2003. Two immunoglobulin G fragment C receptor polymorphisms independently predict response to rituximab in patients with follicular lymphoma. *J. Clin. Oncol.* **21**:3940–3947.
19. Romani, L., et al. 2004. The exploitation of distinct recognition receptors in dendritic cells determines the full range of host immune relationships with *Candida albicans*. *Int. Immunol.* **16**:149–161.
20. Shaw, D.R., and Griffin, F.M., Jr. 1981. Phagocytosis requires repeated triggering of macrophage phagocytic receptors during particle ingestion. *Nature.* **289**:409–411.
21. Dhodapkar, K.M., et al. 2005. Selective blockade of inhibitory Fcγ receptor enables human dendritic cell maturation with IL-12p70 production and immunity to antibody coated tumor cells. *Proc. Natl. Acad. Sci. U. S. A.* **102**:2910–2915.
22. Kalergis, A.M., and Ravetch, J.V. 2002. Inducing tumor immunity through the selective engagement of activating Fcγ receptors on dendritic cells. *J. Exp. Med.* **195**:1653–1659.
23. Mach, P., Serre, K., and Leserman, L. 2000. Class I-restricted presentation of exogenous antigen acquired by Fcγ receptor-mediated endocytosis is regulated in dendritic cells. *Eur. J. Immunol.* **30**:848–857.
24. Yada, A., et al. 2003. Accelerated antigen presentation and elicitation of humoral response in vivo by FcγRIIIB- and FcγRI/III-mediated immune complex uptake. *Cell Immunol.* **225**:21–32.
25. Regnault, A., et al. 1999. Fcγ receptor-mediated induction of dendritic cell maturation and major histocompatibility complex class I-restricted antigen presentation after immune complex internalization. *J. Exp. Med.* **189**:371–380.
26. Selenko, N., et al. 2001. CD20 antibody (C2B8)-induced apoptosis of lymphoma cells promotes phagocytosis by dendritic cells and cross-priming of CD8⁺ cytotoxic T cells. *Leukemia.* **15**:1619–1626.
27. Wolpoe, M.E., et al. 2003. HER-2/neu-specific monoclonal antibodies collaborate with HER-2/neu-targeted granulocyte macrophage colony-stimulating factor secreting whole cell vaccination to augment CD8⁺ T cell effector function and tumor-free survival in Her-2/neu-transgenic mice. *J. Immunol.* **171**:2161–2169.
28. Schuurhuis, D.H., et al. 2002. Antigen-antibody immune complexes empower dendritic cells to efficiently prime specific CD8⁺ CTL responses in vivo. *J. Immunol.* **168**:2240–2246.
29. Schuurhuis, D.H., et al. 2006. Immune complex-loaded dendritic cells are superior to soluble immune complexes as antitumor vaccine. *J. Immunol.* **176**:4573–4580.
30. Dhodapkar, K.M., Krasovsky, J., Williamson, B., and Dhodapkar, M.V. 2002. Antitumor monoclonal antibodies enhance cross-presentation of cellular antigens and the generation of myeloma-specific killer T cells by dendritic cells. *J. Exp. Med.* **195**:125–133.
31. Rafiq, K., Bergtold, A., and Clynes, R. 2002. Immune complex-mediated antigen presentation induces tumor immunity. *J. Clin. Invest.* **110**:71–79.
32. Ercolini, A.M., et al. 2003. Identification and characterization of the immunodominant rat HER-2 MHC class I epitope presented by spontaneous mammary tumors from HER-2/neu-transgenic mice. *J. Immunol.* **170**:4273–4280.
33. Manning, E.A., et al. 2007. A vascular endothelial growth factor receptor-2 inhibitor enhances antitumor immunity through an immune-based mechanism. *Clin. Cancer Res.* **13**:3951–3959.
34. den Haan, J.M., and Bevan, M.J. 2002. Constitutive versus activation-dependent cross-presentation of immune complexes by CD8⁺ and CD8⁻ dendritic cells in vivo. *J. Exp. Med.* **196**:817–827.
35. Dudziak, D., et al. 2007. Differential antigen processing by dendritic cell subsets in vivo. *Science.* **315**:107–111.
36. Burgdorf, S., Kautz, A., Bohnert, V., Knolle, P.A., and Kurtis, C. 2007. Distinct pathways of antigen uptake and intracellular routing in CD4 and CD8 T cell activation. *Science.* **316**:612–616.
37. Akiyama, K., et al. 2003. Targeting apoptotic tumor cells to FcγR provides efficient and versatile vaccination against tumors by dendritic cells. *J. Immunol.* **170**:1641–1648.
38. Winkel, K., Sotzik, F., Vremec, D., Cameron, P.U., and Shortman, K. 1994. CD4 and CD8 expression by human and mouse thymic dendritic cells. *Immunol. Lett.* **40**:93–99.
39. Sallusto, F., Geginat, J., and Lanzavecchia, A. 2004. Central memory and effector memory T cell subsets: function, generation, and maintenance. *Annu. Rev. Immunol.* **22**:745–763.
40. Bonasio, R., and von Andrian, U.H. 2006. Generation, migration and function of circulating dendritic cells. *Curr. Opin. Immunol.* **18**:503–511.
41. Belyakov, I.M., Hammond, S.A., Ahlers, J.D., Glenn, G.M., and Berzofsky, J.A. 2004. Transcutaneous immunization induces mucosal CTLs and protective immunity by migration of primed skin dendritic cells. *J. Clin. Invest.* **113**:998–1007.
42. Enioutina, E.Y., Visic, D., and Daynes, R.A. 2000. The induction of systemic and mucosal immune responses to antigen-adjuvant compositions administered into the skin: alterations in the migratory properties of dendritic cells appears to be important for stimulating mucosal immunity. *Vaccine.* **18**:2753–2767.
43. Mimura, K., et al. 2005. Trastuzumab-mediated antibody-dependent cellular cytotoxicity against esophageal squamous cell carcinoma. *Clin. Cancer Res.* **11**:4898–4904.
44. Guy, C.T., et al. 1992. Expression of the neu protooncogene in the mammary epithelium of transgenic mice induces metastatic disease. *Proc. Natl. Acad. Sci. U. S. A.* **89**:10578–10582.
45. Machiels, J.P., et al. 2001. Cyclophosphamide, doxorubicin, and paclitaxel enhance the antitumor response of granulocyte/macrophage-colony stimulating factor-secreting whole-cell vaccines in HER-2/neu tolerized mice. *Cancer Res.* **61**:3869–3897.
46. Reilly, R.T., et al. 2000. HER-2/neu is a tumor rejection target in tolerized HER-2/neu transgenic mice. *Cancer Res.* **60**:3569–3576.
47. Reilly, R.T., et al. 2001. The collaboration of both humoral and cellular HER-2/neu-targeted immune responses is required for the complete eradication of HER-2/neu-expressing tumors. *Cancer Res.* **61**:880–883.
48. Brechbiel, M.W., et al. 1991. An effective chelating agent for labeling of monoclonal antibody with Bi-212 for a-particle mediated radioimmunotherapy. *J. Chem. Soc. Chem. Commun.* 1169–1170.
49. Nikula, T.K., et al. 1995. A rapid, single vessel method for preparation of clinical grade ligand conjugated monoclonal antibodies. *Nucl. Med. Biol.* **22**:387–390.